Block Copolymers

Deutsche Ausgabe: DOI: 10.1002/ange.201608043
Internationale Ausgabe: DOI: 10.1002/anie.201608043

Exploiting Host–Guest Interactions for the Synthesis of a Rod–Rod Block Copolymer with Crystalline and Liquid-Crystalline Blocks

Feng Zhou, Ke-Hua Gu, Zhen-Yu Zhang, Meng-Yao Zhang, Sheng Zhou, Zhihao Shen, and Xing-He Fan*

Abstract: *By making use of the host–guest interactions between the host molecule tris-o-phenylenedioxycyclotriphosphazene (TPP) and the rod–coil block copolymer (BCP) poly(ethylene oxide)-block-poly(octyl 4′-octyloxy-2-vinylbiphenyl-4-carboxylate) (PEO-b-PVBP), the supramolecular rod–rod block copolymer P(EO@TPP)-b-PVBP was constructed. It consists of a crystalline segment P(EO@TPP) with a hexagonal crystalline structure and a columnar nematic liquid-crystalline segment (PVBP). As the PVBP segments arrange themselves as columnar nematic phases, the crystalline structure of the inclusion complex P(EO@TPP), which has a smaller diameter, is destroyed. The self-assembled nanostructure is thus clearly affected by the interplay between the two blocks. On the basis of wide- and small-angle X-ray scattering analysis, we conclude that the supramolecular rod–rod BCP can self-assemble into a cylinder-in-cylinder double hexagonal structure.*

Block copolymers (BCPs) can be divided into coil–coil, rod–coil, and rod–rod BCPs according to the flexibilities of the two blocks. Rod–rod BCPs, where both blocks are rigid or semi-rigid, have been widely used in electro-optic materials[1] and drug delivery systems,[2] for example. However, compared with coil–coil[3] and rod–coil[4] BCPs, the synthesis of rod–rod BCPs is usually rather complex because the molecular structures of rod blocks are usually more complicated than those of coil ones, which restricts the study and application of rod–rod BCPs. The introduction of supramolecular interactions can solve this problem to some degree, that is, by using supramolecular interactions between small molecules and rod–coil BCPs that can be easily synthesized, we can construct supramolecular rod–rod BCPs. For example, Lee et al. prepared polypseudorotaxane-*block*-poly(γ-benzyl-L-glutamate) supramolecular BCPs by making use of the host–guest interactions between α-cyclodextrins and poly[(ethylene oxide)-*ran*-(propylene oxide)] (P(EO-*r*-PO)) segments in P(EO-*r*-PO)-*block*-poly(γ-benzyl-L-glutamate).[5] Aside from host–guest interactions, other supramolecular interactions, such as electrostatic interactions[6] and hydrogen bonding,[7] have also been introduced to obtain supramolecular BCPs.

Herein, we prepared a supramolecular rod–rod BCP by making use of the the host–guest interactions between tris-*o*-phenylenedioxycyclotriphosphazene (TPP) and the PEO block in the rod–coil BCP PEO-*block*-poly(octyl 4′-octyloxy-2-vinylbiphenyl-4-carboxylate) (PEO-*b*-PVBP). The preparation of the supramolecular BCP P(EO@TPP)-*b*-PVBP is illustrated in Scheme 1. The host molecule TPP, first reported by Allcock and co-workers,[8] can form a channel-type hexagonal crystalline structure, which can trap polymers.[9] TPP molecules are able to recognize and selectively entrap ethylene oxide (EO) sequences in PEO-*b*-PPO-*b*-PEO.[10] Compared to other hosts, the hexagonal crystalline structure of TPP maintains the inclusion crystalline block in good order, which is helpful for building highly organized superstructures. The other rod block PVBP is a mesogen-jacketed liquid-crystalline polymer (MJLCP), which has been shown to be a good candidate for rod blocks.[11] As proposed by Zhou et al., bulky pendants in MJLCPs are considered to be densely packed around the backbone and force it to adopt a rigid or semi-rigid conformation.[12] MJLCPs have been widely used as controllable rod blocks in synthesizing well-defined rod–coil diblock[13] or triblock[14] copolymers and rod–rod BCPs.[15] PVBP can form a columnar nematic (Col_n) liquid-crystalline (LC) phase[16] and has been utilized in our previous study of a covalent rod–rod BCP.[15b] According to our molecular design, the P(EO@TPP)-*b*-PVBP supramolecular rod–rod BCP contains a crystalline segment P(EO@TPP) with a hexagonal crystalline structure and a PVBP-based LC segment with a Col_n phase. Therefore, we can study the interplay between the properties of the LC and crystalline phases along with the effect of such interactions on the self-assembled structure of the supramolecular rod–rod BCP.

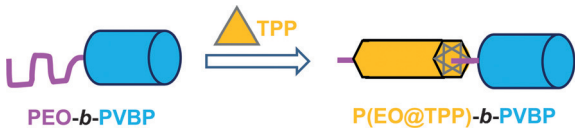

Scheme 1. Schematic representation of the preparation of P(EO@TPP)-*b*-PVBP.

The preparation of the P(EO@TPP)-*b*-PVBP supramolecular rod–rod BCP is illustrated in Scheme 2. Gel permeation chromatography (GPC; see the Supporting Information, Figure S1) and ^{1}H NMR spectroscopy (Figure S2) were applied to determine the molecular weights

[*] Dr. F. Zhou, K.-H. Gu, Z.-Y. Zhang, M.-Y. Zhang, S. Zhou, Prof. Dr. Z. Shen, Prof. Dr. X.-H. Fan
Beijing National Laboratory for Molecular Sciences
Key Laboratory of Polymer Chemistry and Physics of Ministry of Education, Center for Soft Matter Science and Engineering
College of Chemistry and Molecular Engineering
Peking University, Beijing 100871 (China)
E-mail: zshen@pku.edu.cn

Supporting information for this article can be found under: http://dx.doi.org/10.1002/anie.201608043.

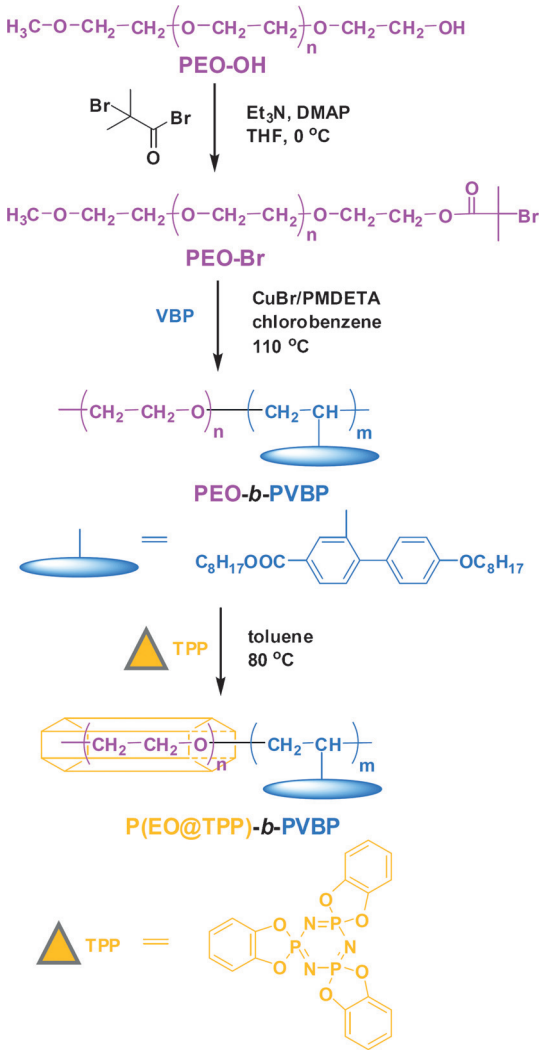

Scheme 2. Synthesis of the P(EO@TPP)-*b*-PVBP supramolecular rod–rod BCP.

and confirm the chemical structures of the PEO-*b*-PVBP BCPs (see Table S1). The host molecule TPP was synthesized according to reported methods[8,10] and characterized by mass spectrometry and elemental analysis (EA; for details see the Experimental Section in the Supporting Information).

Before the preparation of the supramolecular rod–rod BCPs, we first determined a suitable EP/TPP molar ratio for the formation of the inclusion complex (IC) by using TPP and the PEO homopolymer (see the Supporting Information for details). According to these studies, EO and TPP should be employed in a molar ratio of about 1.3:1. P(EO@TPP)-*b*-PVBP was then prepared from a toluene solution of PEO-*b*-PVBP and TPP at a EO/TPP ratio of 1.3:1. ^{13}C solid-state NMR spectroscopy (Figure 1) was used to confirm the chemical structure of the supramolecular rod–rod BCP. For the TPP crystal, there are three main peaks at 145, 125, and 113 ppm, which indicates that TPP has a hexagonal crystalline structure instead of a monoclinic crystalline phase, which would give rise to more complicated resonances in the NMR spectrum.[17] In the spectrum of P(EO@TPP)$_{46}$-*b*-PVBP$_{86}$,

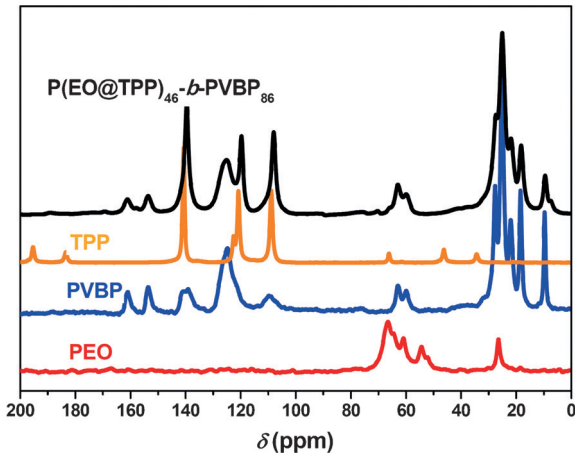

Figure 1. ^{13}C solid-state NMR spectra of PEO, PVBP, TPP, and P-(EO@TPP)$_{46}$-*b*-PVBP$_{86}$.

there are three resonances at the corresponding positions, indicating that the P(EO@TPP) segment in the supramolecular BCP also exhibits the hexagonal crystalline structure.

In P(EO@TPP)-*b*-PVBP, the crystalline block exhibits a hexagonal crystalline structure with a unit cell parameter $a = 1.14$ nm whereas the PVBP block can form a Col$_n$ LC phase with a rod diameter of 1.87 nm at high temperatures.[9b,16] We first examined the interplay between the arrangements of the two blocks. Figure 2a shows wide-angle X-ray scattering (WAXS) profiles of P(EO@TPP)$_{46}$-*b*-PVBP$_{86}$ at different temperatures. The scattering halo with $q = 3.20$ nm^{-1} can be attributed to the packing of the PVBP rod-like chains, and the diffraction peaks with q values of 6.15, 8.70, 12.30, and 13.73 nm^{-1} correspond to the (100), (101), (200), and (201) diffractions of the hexagonal crystal of P(EO@TPP)$_{46}$. Upon heating, the scattering halo of PVBP does not change much, which indicates that the PVBP$_{86}$ block does not form an LC phase even at 200 °C. At the same time, the intensities of the diffraction peaks of P(EO@TPP)$_{46}$ decrease, indicating that the hexagonal crystal is partially destroyed during the heating process. To confirm the above conjecture, we isothermally treated the sample at 200 °C for 8 h. As shown in Figure S5, the scattering halo of PVBP does not change while the characteristic diffractions of P(EO@TPP) almost disappear. These results demonstrate that the P(EO@TPP) crystal is destroyed at temperatures much lower than its T_m even though the PVBP segment does not form an LC phase. As PVBP has a larger rod diameter (1.87 nm), the trend for the PVBP macromolecular chains to be packed together during the heating process affects the crystalline packing of P(EO@TPP) with a smaller size (1.14 nm). A similar phenomenon was observed in our previous studies on rod–rod BCPs with different rod diameters, where there was an imbalance between the interfacial areas of the two rods.[15b]

The WAXS profiles of P(EO@TPP)$_{46}$-*b*-PVBP$_{121}$ during heating are shown in Figure 2b. The scattering halo of PVBP at $q = 3.20$ nm^{-1} turns into a sharp diffraction peak when the sample is heated to 160 °C; at this temperature, the diffraction peak with $q = 3.35$ nm^{-1} (corresponding to a *d*-spacing of

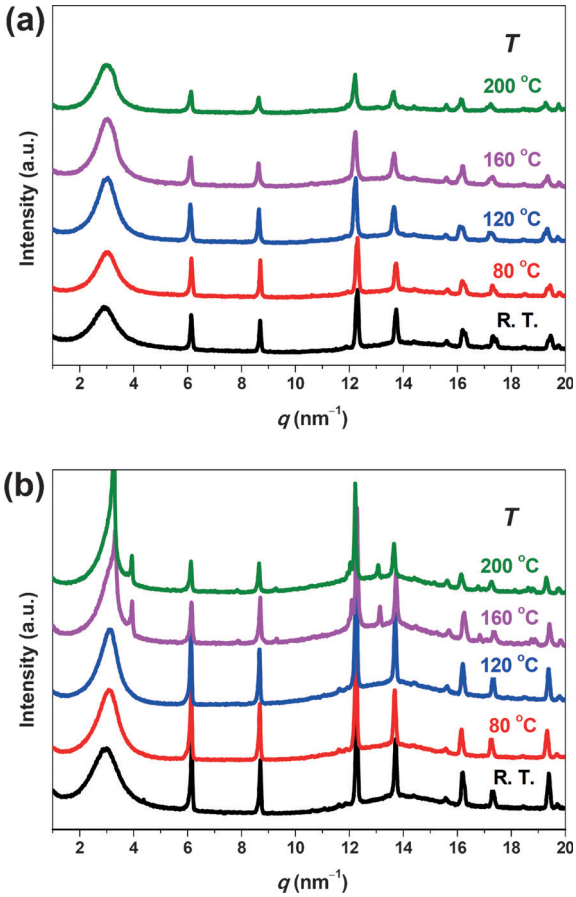

Figure 2. WAXS profiles of a) P(EO@TPP)$_{46}$-*b*-PVBP$_{86}$ and b) P-(EO@TPP)$_{46}$-*b*-PVBP$_{121}$ during heating.

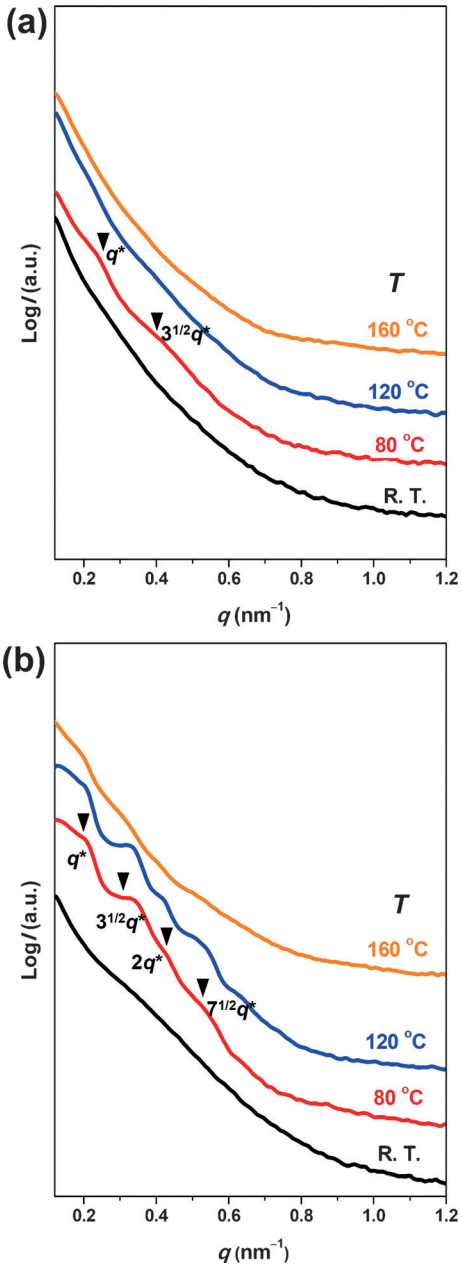

Figure 3. SAXS profiles of a) P(EO@TPP)$_{46}$-*b*-PVBP$_{86}$ and b) P-(EO@TPP)$_{46}$-*b*-PVBP$_{121}$ during heating.

1.87 nm) can be attributed to the Col$_n$ phase of PVBP. On the other hand, several new peaks at $q = 3.94$, 7.88, 9.30, and 13.14 nm^{-1} (originating from the monoclinic structure of TPP)[10] appeared at 160 °C, indicating that the hexagonal crystalline structure is partially destroyed and transformed into a monoclinic phase. The above results demonstrate that the formation of the Col$_n$ phase of PVBP$_{121}$ causes more disturbances to the hexagonal crystalline structure of P-(EO@TPP)$_{46}$ compared with the influence of amorphous PVBP. The results in Figure 2 confirm that there is competition between the arrangements of the two rods and that the packing of the PVBP rods with a larger diameter destroys the hexagonal structure of the P(EO@TPP) rods.

The interplay between the two rod blocks is expected to affect the microphase-separated nanostructure of the BCP. The nanostructures were determined by small-angle X-ray scattering (SAXS) experiments (Figure 3). For P-(EO@TPP)$_{46}$-*b*-PVBP$_{86}$ (Figure 3a), there is no diffraction peak at ambient temperature. After the sample had been heated to 80 °C, there were two diffraction peaks with a scattering vector ratio of $1/3^{1/2}$, characteristic of a hexagonally packed cylindrical (HEX) structure. However, once the temperature was increased to 160 °C, the two diffraction peaks disappeared, suggesting that the BCP becomes disordered. For P(EO@TPP)$_{46}$-*b*-PVBP$_{121}$ (Figure 3b), there are four diffraction peaks with a scattering vector ratio of $1/3^{1/2}/2/7^{1/2}$ at 80 °C, also indicating a HEX structure. Similar to P(EO@TPP)$_{46}$-*b*-PVBP$_{86}$, it was difficult to recognize the diffractions corresponding to the HEX nanostructure when the temperature reached 160 °C, implying that the ordered structure had been destroyed. In combination with the WAXS results (Figure 2), which showed that the hexagonal packing of P(EO@TPP) is destroyed at 160 °C, we conclude that the ordered microphase-separated structure becomes disordered following the disappearance of the hexagonal crystalline structure of P(EO@TPP) owing to the competition between the different arrangements of the two rods. The weight fractions of PVBP (w_{PVBP}) are about 69% and 75% for P(EO@TPP)$_{46}$-*b*-PVBP$_{86}$ and P(EO@TPP)$_{46}$-*b*-PVBP$_{121}$, respectively, on the basis of the molecular weights of the

two components in the rod–rod BCPs. Therefore, it is reasonable to assume that the supramolecular rod–rod BCPs form HEX nanostructures with PVBP as the continuous phase. The microphase-separated nanostructures of the supramolecular rod–rod BCP at different temperatures are illustrated in Figure 4. The proposed structure is similar to the cylinder-in-cylinder morphologies reported for some rod–coil[18] and rod–rod[15a] BCPs, with the difference being that the P(EO@TPP) segment possesses a crystalline structure in the supramolecular rod–rod BCP.

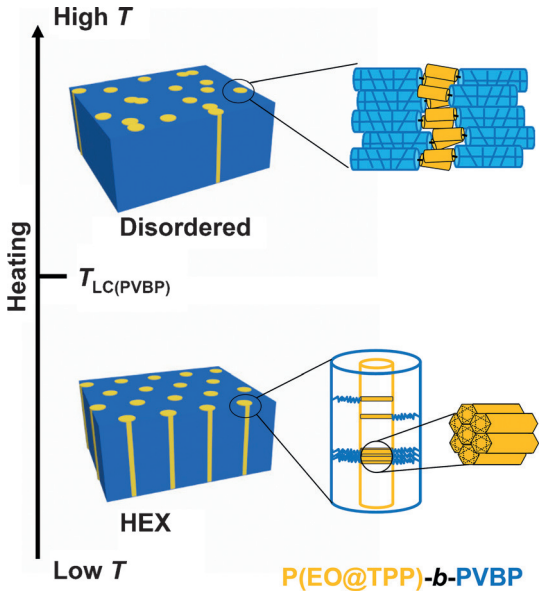

Figure 4. Illustration of the microphase-separated nanostructure of the supramolecular rod–rod BCP at different temperatures. The PVBP block is amorphous at low temperatures and liquid crystalline at high temperatures.

As indicated by the results in Figures 2 and 3, the hexagonal crystalline structure of P(EO@TPP) is formed at ambient temperature and remains unchanged when the temperature is lower than 160 °C. Meanwhile, the PVBP block does not form an LC phase below 160 °C and can be considered to have some flexibility at temperatures above its glass transition temperature (T_g) of 45 °C.[16] Therefore, the higher degree of molecular motion of the PVBP chains leads to the formation of the ordered BCP HEX nanostructure. When the temperature reaches the LC formation temperature ($T_{LC} \approx 160$ °C as indicated in Figure 2b) of PVBP, the PVBP block forms a Col_n LC phase with a rod diameter of 1.87 nm, which is significantly larger than the diameter (1.14 nm, which is also the unit cell parameter of the hexagonal crystalline structure) of P(EO@TPP). Moreover, the packings of these two blocks are also different. Thus the crystal packing of P(EO@TPP) is destroyed owing to the competition between the different arrangements of these two rods, resulting in the destruction of the self-assembled structure of the supramolecular rod–rod BCP. For the self-assembly of BCPs, the areas of the interfaces between the two segments greatly influence the packing of the blocks and the resultant phase diagrams.[13c,15b] Evidently, there is an imbalance between the interfacial areas of PVBP and P(EO@TPP), resulting in the disruption of the self-assembled ordered structures. As a result, we propose that when a crystalline rod and an LC rod are combined in one BCP, the interplay between them determines the self-assembled structure of the supramolecular rod–rod BCP.

In conclusion, we have constructed a supramolecular rod–rod block copolymer, P(EO@TPP)-*b*-PVBP, by making use of the host–guest interactions between the host molecule TPP and the rod–coil BCP PEO-*b*-PVBP. In P(EO@TPP)-*b*-PVBP, the P(EO@TPP) block has a hexagonal crystalline structure whereas the PVBP block can form a Col_n LC phase at high temperatures. The differences in the arrangements and the diameters of the two rod-like segments lead to competition between the packings of the two rods. The formation of the Col_n phase of PVBP destroys the hexagonal crystalline structure of P(EO@TPP), and the self-assembled nanostructure is also destroyed at the same time. According to our WAXS and SAXS results, the supramolecular rod–rod BCP can self-assemble into a cylinder-in-cylinder double hexagonal structure. As crystals are more convenient starting materials to construct three-dimensionally ordered structures, the supramolecular rod–rod BCP in this work is of potential use in the preparation of two- and three-dimensionally ordered nanomaterials with hierarchical structures.

Acknowledgements

This work was supported by the National Natural Science Foundation of China (Grants 21174006 and 51473005).

Keywords: block copolymers · liquid crystals · host–guest interactions · self-assembly · supramolecular chemistry

How to cite: *Angew. Chem. Int. Ed.* **2016**, *55*, 15007–15011
Angew. Chem. **2016**, *128*, 15231–15235

[1] a) U. Scherf, S. Adamczyk, A. Gutacker, N. Koenen, *Macromol. Rapid Commun.* **2009**, *30*, 1059–1065; b) S.-S. Sun, C. Zhang, A. Ledbetter, S. Choi, K. Seo, J. C. E. Bonner, *Appl. Phys. Lett.* **2007**, *90*, 043117.
[2] E. G. Bellomo, M. D. Wyrsta, L. Pakstis, D. J. Pochan, T. J. Deming, *Nat. Mater.* **2004**, *3*, 244–248.
[3] A. K. Khandpur, S. Foerster, F. S. Bates, I. W. Hamley, A. J. Ryan, W. Bras, K. Almdal, K. Mortensen, *Macromolecules* **1995**, *28*, 8796–8806.
[4] M. Lee, B.-K. Cho, W.-C. Zin, *Chem. Rev.* **2001**, *101*, 3869–3892.
[5] H.-F. Lee, H.-S. Sheu, U. S. Jeng, C.-F. Huang, F.-C. Chang, *Macromolecules* **2005**, *38*, 6551–6558.
[6] a) C. Li, J. Li, X. Zhang, A. Zhang, R. Mezzenga, *Macromol. Rapid Commun.* **2010**, *31*, 265–269; b) J. S. Haataja, N. Houbenov, H. Iatrou, N. Hadjichristidis, A. Karatzas, C. F. J. Faul, P. Rannou, O. Ikkala, *Biomacromolecules* **2012**, *13*, 3572–3580.
[7] a) E. Weiss, K. C. Daoulas, M. Müller, R. Shenhar, *Macromolecules* **2011**, *44*, 9773–9781; b) J.-X. Yang, B. Fan, J.-H. Li, J.-T. Xu, B.-Y. Du, Z.-Q. Fan, *Macromolecules* **2016**, *49*, 367–372; c) S.-W. Kuo, P.-H. Tung, C.-L. Lai, K.-U. Jeong, F.-C. Chang, *Macromol. Rapid Commun.* **2008**, *29*, 229–233; d) S.-W. Kuo, *Polym. Int.* **2009**, *58*, 455–464.

[8] H. R. Allcock, M. L. Levin, R. R. Whittle, *Inorg. Chem.* **1986**, *25*, 41 – 47.
[9] a) A. P. Primrose, M. Parvez, H. R. Allcock, *Macromolecules* **1997**, *30*, 670 – 672; b) H. R. Allcock, A. P. Primrose, N. J. Sunderland, A. L. Rheingold, I. A. Guzei, M. Parvez, *Chem. Mater.* **1999**, *11*, 1243 – 1252.
[10] S. Bracco, A. Comotti, L. Ferretti, P. Sozzani, *J. Am. Chem. Soc.* **2011**, *133*, 8982 – 8994.
[11] X.-F. Chen, Z. Shen, X.-H. Wan, X.-H. Fan, E.-Q. Chen, Y. Ma, Q.-F. Zhou, *Chem. Soc. Rev.* **2010**, *39*, 3072 – 3101.
[12] a) Q. F. Zhou, H. M. Li, X. D. Feng, *Macromolecules* **1987**, *20*, 233 – 234; b) Q. F. Zhou, X. L. Zhu, Z. Q. Wen, *Macromolecules* **1989**, *22*, 491 – 493.
[13] a) Y. F. Tu, X. H. Wan, D. Zhang, Q. F. Zhou, C. Wu, *J. Am. Chem. Soc.* **2000**, *122*, 10201 – 10205; b) C. Y. Li, K. K. Tenneti, D. Zhang, H. L. Zhang, X. H. Wan, E. Q. Chen, Q. F. Zhou, A. O. Carlos, S. Igos, B. S. Hsiao, *Macromolecules* **2004**, *37*, 2854 – 2860; c) K. K. Tenneti, X. Chen, C. Y. Li, Y. Tu, X. Wan, Q.-F. Zhou, I. Sics, B. S. Hsiao, *J. Am. Chem. Soc.* **2005**, *127*, 15481 – 15490; d) L.-Y. Shi, Y. Zhou, X.-H. Fan, Z. Shen, *Macromolecules* **2013**, *46*, 5308 – 5316.
[14] a) L. Gao, J. Yao, Z. Shen, Y. Wu, X. Chen, X. Fan, Q. Zhou, *Macromolecules* **2009**, *42*, 1047 – 1050; b) L.-C. Gao, X.-H. Fan, Z.-H. Shen, X. Chen, Q.-F. Zhou, *J. Polym. Sci. Part A* **2009**, *47*, 319 – 330; c) L.-Y. Shi, Y. Pan, Q.-K. Zhang, Y. Zhou, X.-H. Fan, Z.-H. Shen, *Chin. J. Polym. Sci.* **2014**, *32*, 1524 – 1534.
[15] a) Q.-H. Zhou, J.-K. Zheng, Z. Shen, X.-H. Fan, X.-F. Chen, Q.-F. Zhou, *Macromolecules* **2010**, *43*, 5637 – 5646; b) F. Zhou, T. Ye, L. Shi, C. Xie, S. Chang, X. Fan, Z. Shen, *Macromolecules* **2013**, *46*, 8253 – 8263; c) F. Zhou, Q.-H. Zhou, H.-J. Tian, C.-S. Li, Y.-D. Zhang, X.-H. Fan, Z.-H. Shen, *Chin. J. Polym. Sci.* **2015**, *33*, 709 – 720.
[16] L. Zhang, H. Wu, Z. Shen, X. Fan, Q. Zhou, *J. Polym. Sci. Part A* **2011**, *49*, 3207 – 3217.
[17] C. Angiolina, S. Roberto, S. Sonia, S. Piero, *Nanotechnology* **1999**, *10*, 70 – 76.
[18] a) H.-A. Klok, J. F. Langenwalter, S. Lecommandoux, *Macromolecules* **2000**, *33*, 7819 – 7826; b) W.-N. He, J.-T. Xu, *Prog. Polym. Sci.* **2012**, *37*, 1350 – 1400.

Received: August 17, 2016
Revised: September 28, 2016
Published online: October 26, 2016

